

Investigation of a Conductivity Logging Tool Based on Single Coil Impedance Measurement Using FDTD Method

Shiwei Sheng, Kang Li*, Fanmin Kong, and Bin Wang

Abstract—Eddy current test has been widely used in many fields because of its simplicity and robustness. In this paper, numerical simulations based on the finite-difference time-domain method were carried out to validate if the eddy current coil can effectively be used in the logging while drilling system. The simulation results showed that the impedance of the eddy current coil is a function of conductivity of the surrounding media. The formation conductivity is strongly dependent on the concentration of hydrocarbons, so different formation layers can be distinguished by measuring coil impedance. Different source frequencies were applied, and it was found that this method works well in frequency range from 100 MHz to 1 GHz. The investigation depth was studied in this paper, and a 3-layer formation model was simulated in this paper. The results showed that this novel method could be effectively used in a well logging system.

1. INTRODUCTION

The detection of oil and gas resources has become more and more important because of the decrease of petroleum reserves after hundred of years of drilling [1]. Many works have been done by laboratories and research institutes in recent years regarding the resistivity and permittivity of formations [2–4]. Logging while drilling (LWD) sensors are widely used in real-time borehole measurements of petrophysical parameters for hydrocarbon exploration [5]. In LWD systems, conductivity (resistivity) of formation is one of the basic indicators of the concentration of hydrocarbon saturation [6, 7]. The conductivity tools measure the conductivity of formation near the bore-hole to determine the rock porosity and water saturation, which are essential for the detection of oil distribution [8]. We know that when the drill is in the water layer or rock layer, drilling fluid salinity is relatively high, and therefore the conductivity will be relatively high. On the other hand, when the drill is in the oil or gas layer, the conductivity will be relatively low. As a result, the oil, gas and water layer distribution can be distinguished by measuring conductivity of the formation. In applications, conductivity of rock often varies from 0.1 to 5 S/m, and water varies from 1 to 15 S/m. Typical commercial electromagnetic propagation tools (EPT) usually adopt coil arrays to measure the conductivity of formation for eliminating the bore-hole effect [7, 8]. For example, one transmitting coil and two receiving coils are assembled in one system. The amplitude difference and phase shift between the two receiving coils can be measured, and hence according to Eq. (1) and Eq. (2), electromagnetic properties of the formation can be deduced [7].

$$\varepsilon = \frac{\alpha^2 - \beta^2}{\omega^2 \mu} \quad (1)$$

$$\sigma = \frac{2\alpha\beta}{\omega\mu} \quad (2)$$

where ε is the permittivity, σ the resistivity, β the phase shift per meter, α the attenuation per meter, ω the frequency, and μ the magnetic permeability.

Received 19 September 2014, Accepted 6 November 2014, Scheduled 14 November 2014

* Corresponding author: Kang Li (kangli@sdu.edu.cn).

The authors are with the School of Information Science and Engineering, ShanDong University, Jinan 250100, China.

Meanwhile, eddy current test (ECT) has been widely used in many application fields including non-destructive testing, distance measurement, and material properties measurement. It is thought that the eddy current coil can also be used in the well-logging system [9]. The theory of ECT is that the impedance of coil is relevant to the conductivity of device under test. Some groups studied the use of eddy current coil to characterize double metal layer, and accurate estimates of the thickness and conductivity of the metal layer can be obtained from measurements of the impedance of the coil. Other researchers studied the impedance of the coil covering layered metal plates [10–12], over an infinite metallic half space [13], or at the opening of a borehole in a conductor [14]. Moreover, a simplified analytical impedance model for a simple single turn eddy current sensor including measurement and parasitic effect has been given recently [15]. Work of [16, 17] developed a method to use the eddy current coil to measure the electromagnetic properties and inner diameter of an oil tube. However, much less is known about the eddy-current coil's impedance when being used in oil well-logging environment.

The purpose of this research is to validate the feasibility of a method which measuring the conductivity of the formation in a simpler way — by measuring the impedance of a coil. This method can eventually increase the robustness of the conductivity measurement system working for LWD system. In general, finite difference method and finite element method are employed for three-dimensional numerical modeling of the LWD tools [8, 18]. Here, to validate this novel method, we conducted a series of finite-difference time-domain (FDTD) simulations to calculate the impedance of a coil in the down-hole environment. In this paper, we briefly described the method how impedance of the copper coil was extracted through the FDTD calculated \mathbf{E} field and \mathbf{H} field. Accuracy of the simulations has been verified through examples. The coil in the down-hole environment was simulated, and it was found that the eddy current coil could be used to obtain the conductivity of the formation. We also studied the investigation depth of this method at different operating frequencies, and a traditional 3-layer formation well-logging example was simulated. The results showed that the method had well applicability for LWD applications, and this work is meaningful for providing reference in well logging field.

2. NUMERICAL METHODS

In this paper, three-dimensional electromagnetic field distributions were calculated using the FDTD method, which is a space and time discretization of Maxwell curl equations [19]:

$$\varepsilon_r \varepsilon_0 \frac{\partial \mathbf{E}}{\partial t} = \nabla \times \mathbf{H} \quad (3)$$

$$\mu_0 \frac{\partial \mathbf{H}}{\partial t} = -\nabla \times \mathbf{E} \quad (4)$$

the above Maxwell curl equations are discretized as follow equations:

$$\begin{aligned} E_x^{n+1}(i+1/2, j, k) &= ca(i+1/2, j, k) \cdot E_x^{n-1/2}(i+1/2, j, k) \\ &+ cb(i+1/2, j, k) \cdot \left[\begin{aligned} &H_z^{n+1/2}(i+1/2, j+1/2, k) - H_z^{n+1/2}(i+1/2, j-1/2, k) \\ &- H_y^{n+1/2}(i+1/2, j, k+1/2) + H_y^{n+1/2}(i+1/2, j, k-1/2) \end{aligned} \right] \end{aligned} \quad (5)$$

$$\begin{aligned} E_y^{n+1}(i, j+1/2, k) &= ca(i, j+1/2, k) \cdot E_y^n(i, j+1/2, k) \\ &+ cb(i, j+1/2, k) \cdot \left[\begin{aligned} &H_x^{n+1/2}(i, j+1/2, k+1/2) - H_x^{n+1/2}(i, j+1/2, k-1/2) \\ &- H_z^{n+1/2}(i+1/2, j+1/2, k) + H_z^{n+1/2}(i-1/2, j+1/2, k) \end{aligned} \right] \end{aligned} \quad (6)$$

$$\begin{aligned} E_z^{n+1}(i, j, k+1/2) &= ca(i, j, k+1/2) \cdot E_z^{n-1/2}(i, j, k+1/2) \\ &+ cb(i, j, k+1/2) \cdot \left[\begin{aligned} &H_y^{n+1/2}(i+1/2, j, k+1/2) - H_y^{n+1/2}(i-1/2, j, k+1/2) \\ &- H_x^{n+1/2}(i, j+1/2, k+1/2) + H_x^{n+1/2}(i-1, j-1/2, k+1/2) \end{aligned} \right] \end{aligned} \quad (7)$$

$$H_x^{n+1/2}(i, j+1/2, k+1/2) = cp(i, j+1/2, k+1/2) \cdot H_x^{n-1/2}(i, j+1/2, k+1/2) \\ + cq(i, j+1/2, k+1/2) \cdot \begin{bmatrix} E_y^n(i, j+1/2, k+1) - E_y^n(i, j+1/2, k) \\ -E_z^n(i, j+1, k+1/2) + E_z^n(i, j, k+1/2) \end{bmatrix} \quad (8)$$

$$H_y^{n+1/2}(i+1/2, j, k+1/2) = cp(i+1/2, j, k+1/2) \cdot H_y^{n-1/2}(i+1/2, j, k+1/2) \\ + cq(i+1/2, j, k+1/2) \cdot \begin{bmatrix} E_z^n(i+1, j, k+1/2) - E_z^n(i, j, k+1/2) \\ -E_x^n(i+1/2, j, k+1) + E_x^n(i+1/2, j, k) \end{bmatrix} \quad (9)$$

$$H_z^{n+1/2}(i+1/2, j+1/2, k) = cp(i+1/2, j+1/2, k) \cdot H_z^{n-1/2}(i+1/2, j+1/2, k) \\ + cq(i+1/2, j+1/2, k) \cdot \begin{bmatrix} +E_x^n(i+1/2, j+1, k) - E_x^n(i+1/2, j, k) \\ -E_y^n(i+1, j+1/2, k) + E_y^n(i, j+1/2, k) \end{bmatrix} \quad (10)$$

where ca , cb , cp , cq are parameters determined by:

$$ca = \frac{1 - \left(\frac{\sigma \cdot \Delta t}{2\varepsilon_r \varepsilon_0}\right)}{1 + \left(\frac{\sigma \cdot \Delta t}{2\varepsilon_r \varepsilon_0}\right)}, \quad cb = \frac{1}{2\varepsilon_r \varepsilon_0 c_0}, \quad cp = 1, \quad cq = \frac{1}{2\mu_0 c_0} \quad (11)$$

where ε_r and σ are the permittivity and conductivity respectively. ε_0 is the free space dielectric constant, μ_0 the magnetic permeability, c_0 the speed of light in vacuum, and Δt the time step of FDTD method. However, FDTD analysis only provides full-vector \mathbf{E} and \mathbf{H} fields. Therefore, to get the impedance of the coil, the following fundamental expressions can be used [19, 20]:

$$V = \int_{Cv} \mathbf{E} \cdot d\mathbf{l} \quad (12)$$

$$I = \oint_{Cl} \mathbf{H} \cdot d\mathbf{l} \quad (13)$$

Here, Cv is the line path extending from a defined voltage reference point and Cl a contour wrap completely around the coil wire at its surface. So, voltage in FDTD can be easy to get by the line integration from one endpoint to the other endpoint of the coil:

$$V = \sum E_{x_i} \cdot \Delta x_i \quad (14)$$

And the current through a point in the wire in x direction can be calculated by:

$$I_x = [H_z(i+1/2, j+1/2, k) - H_z(i+1/2, j-1/2, k)] \cdot \Delta z \\ + [H_y(i+1/2, j, k-1/2) - H_y(i+1/2, j, k+1/2)] \cdot \Delta y \quad (15)$$

So, the current through the wire can be calculated by the sum of the currents in points within the transverse profile:

$$I = \sum I_x \quad (16)$$

After a few calculation steps, the coil impedance as a function of frequency can be obtained from:

$$Z(\omega) = \frac{fft[V(t)]}{fft[I(t)]} \quad (17)$$

Before calculating the impedance of the coil in the formation, we first checked the accuracy of our simulation method. As an example for simplicity, we simulated a coil in the air, and the 3D model of the coil is shown as Figure 1. The excitation source was placed between the two ends of the coil. The material of the coil was copper. The conductivity of copper was set as $5.8e+7$ S/m and the permittivity set as 1. The coil diameter was 10 cm, and the wire diameter varied from 1 mm to 4 mm. Usually, FDTD simulation uses a sinusoidal source, and it usually needs long time to achieve convergence. To reduce the simulation time consumption, we used a ramp sinusoidal signal as the excitation. The FDTD cells of the coil were sized as $\Delta x = \Delta y = \Delta z = 0.5$ mm to ensure accuracy. Perfect matched layer (PML),

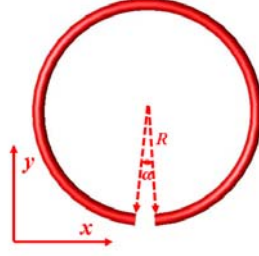


Figure 1. Three-dimensional schematic view of a one-turn eddy current coil, this coil was placed in the air. The material of the coil is copper, and the angle α of the gap for adding excitations source is 5° .

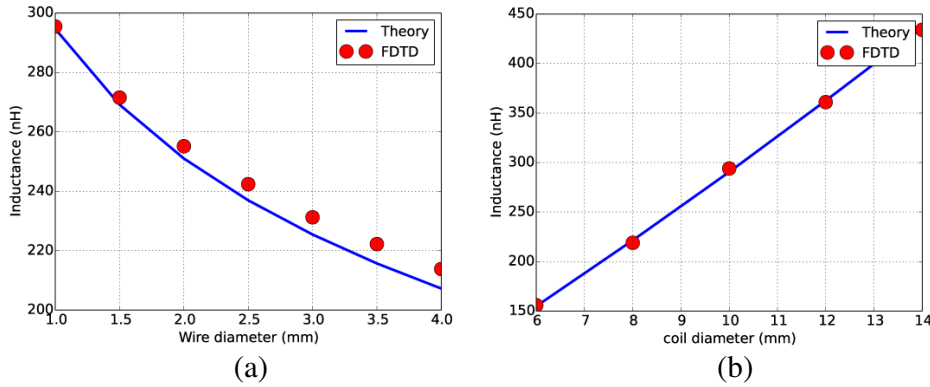


Figure 2. Comparison of the FDTD calculated value of inductance vs. the analytic values of Eq. (18) (a) with wire diameters vary from 1 mm to 4 mm; (b) with coil diameters vary from 6 cm to 14 cm.

which was 10 cells thick, was employed for the FDTD simulation scheme. The theoretical formula to calculate the inductor of single metal loop in the air is given by [21]:

$$L = 0.01595D \left(2.303 \log_{10} \frac{8D}{d} - 2 + \mu\delta \right) \quad (18)$$

where D is the diameter of the coil, d the diameter of the wire (both are in inches), μ the permeability of the coil, and δ the skin effect depth, which is a frequency related value and can be find in [21]. We know that the impedance of a coil can be termed as $Z(\omega) = (R_r + R_L) + j\omega L(\Omega)$, where R_r is the radiation resistance of the coil, R_L the loss resistance of the coil, and L the inductance of the coil. As a result, the inductance of the eddy current coil in the air can be obtained through the reactance part of FDTD calculated impedance:

$$L = \text{Im}(Z(\omega)) / (2\pi f) \quad (19)$$

All the FDTD calculation results and analytical calculation results using Eq. (18) are plotted in Figure 2(a), and the deviations are shown in Table 1. We can see that in all cases, the FDTD calculated value is within 3% of the analytic value. We also simulated another example where the coil diameter varied from 6 cm to 14 cm, and the wire diameter was constant at 1 mm. These results are shown in Figure 2(b), and the deviations are shown in Table 2. In all cases, the FDTD calculated value is within 2% of the analytic value.

3. CALCULATION AND DISCUSSION

3.1. Coil Impedance Along with the Formation Conductivity

First, we investigated the influence of the formation conductivity on the coil's impedance. A simulation of a copper coil (with 20 turns, wire diameter of 4 mm and coil diameter of 70 mm) was put in the

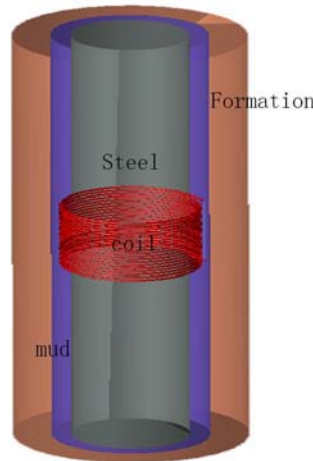


Figure 3. 3D model of an 20 turn coil in a bore-hole environment. The wire diameter of the coil is 4 mm and coil diameter is 7 cm. This coil was directly dipped in the drilling liquid.

Table 1. Deviation of FDTD calculated value when wire diameter varies from 1 mm to 4 mm.

Wire diameter	Deviation
1.0	0.27%
1.5	0.90%
2.0	1.62%
2.5	2.40%
3.0	2.50%
3.5	2.93%
4.0	3.00%

Table 2. Deviation of FDTD calculated value when coil diameter varies from 6 cm to 14 cm.

Coil diameter	Deviation
6	1.41%
8	0.30%
10	1.91%
12	0.30%
14	0.10%

down-hole environment. The coil was directly dipped in the drilling mud. The three-dimensional model of this simulation is shown in Figure 3, where the steel diameter was set as 60 mm, the well bore diameter 80 mm, the horizontal depth of ground formation 200 mm, and the vertical depth of ground formation 1 m. To ensure accuracy, the FDTD cell size of the coil was set as $\Delta x = \Delta y = \Delta z = 0.5$ mm. Also, PML with 10 cells thick was applied in this simulation. In many works, these conductivities of formations are anisotropic because of geological factors such as the presence of sand and clay laminates with directional resistivities or the presence of salt water in fractured porous formations. However, for ease and simplicity, here we use homogeneous isotropy media in the simulations. And in a real well logging system, formation conductivity usually varies within 0 to 10 S/m, so in this simulation, the earth formation conductivity was set to vary from 0 to 10 S/m. As shown in Table 3, the formation relative permittivity was set at 10. The conductivity of drilling mud was 2 S/m, and the relative permittivity was 20. Different operating frequencies from 10 MHz to 10 GHz were calculated. When using induction tools operating at low frequency or electrode tools, the mud used is often water-based, which can cause very deep invasion. However, when EPT operating at high frequency, the mud used is often oil-based, and the invasion is very shallow and can be neglected especially in a real time operating LWD system, so, the invasion and well bore effect was neglected in this simulation.

Figure 4 shows the response of the tool at different frequencies as a function of different formation conductivities. We can see that when frequency is in 10 MHz, the real and imaginary parts of impedance keep nearly same as the formation conductivity increase, and the variation of the impedance is less than one Ohm. As mentioned before, the impedance of a coil can be termed as $\text{Real}(Z(\omega)) = (R_r + R_L)$. We know that R_L of copper coil is very small, and this means that at lower frequency, radiation resistance of the coil at down hole environment is also small. And because the imaginary part of the impedance is a frequency related value, the lower operating frequency will cause a small value. When frequency

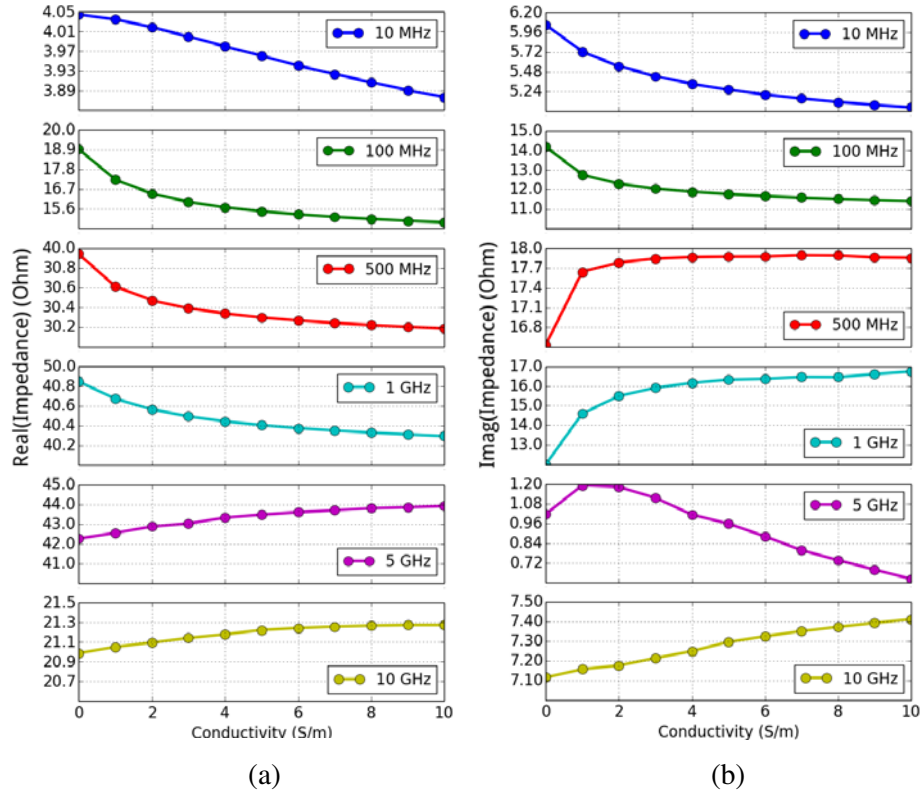


Figure 4. (a) real part and (b) imaginary part of impedance along with the increase of conductivity at different operating frequencies.

Table 3. Electric and magnetic parameters for model plotted in Figure 3.

Material	Conductivity (S/m)	Permittivity
Formation	0–10	10
Mud	2	20
Steel	1.04e7	1
Coil	5.80e7	1

is in 100 MHz, both the real and imaginary parts of impedance decrease as the formation conductivity increases. When frequency is in 500 MHz and 1 GHz, the real part of the impedance decreases, and the imaginary part increases as the formation conductivity increases. But when the frequency is up to 5 GHz, those relationships vanish, the variation of impedance as the formation conductivity increase becomes very small again. This is caused by the shallow penetration depth of the tool when operating at high frequency. Actually, in traditional EPT logging, the operation frequencies are between 10 MHz to 2 GHz. If the frequency is higher than 2 GHz, the depth of investigation will become too small to be useful, which is in coincidence with our results.

3.2. Investigation Depth in Different Frequencies

As high frequency can cause very shallow investigation depth, it is necessary to evaluate the investigate depth of this method operating at different frequencies. In next simulation, we changed the well bore diameters from 80 mm to 100 mm (means drilling mud depth varies from 2 cm to 4 cm). The 3D model used and other FDTD settings were the same as before. The operating frequencies were chosen as 100 MHz, 500 MHz and 1 GHz. Figures 5(a)–(f) show the FDTD calculated results that as well bore diameter increases, both the real and imaginary parts of the impedance vary less. When the well

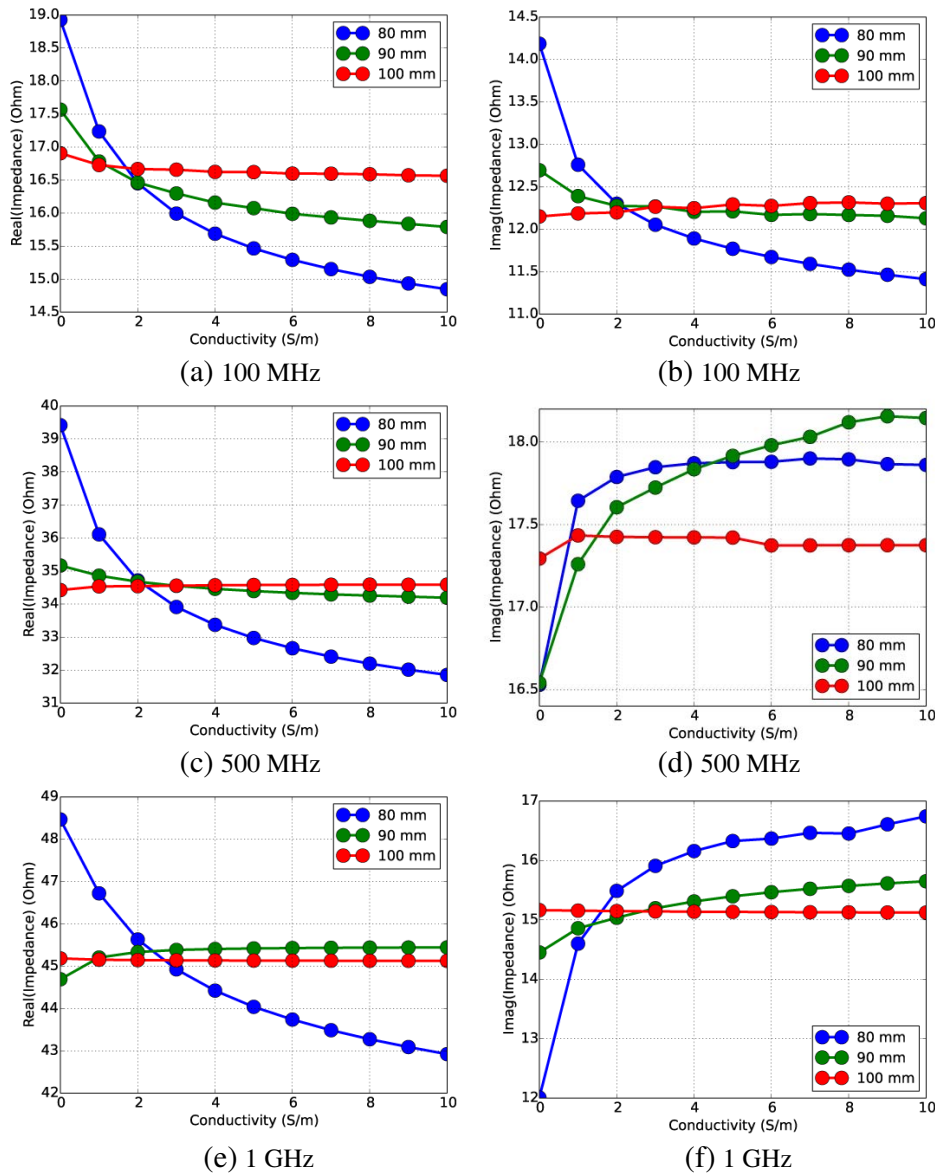


Figure 5. (a), (c), (e) are the real part and (b), (d), (f) are imaginary part of impedance along with the increase of conductivity at different well bore diameters in different frequencies.

bore diameter is 100 mm, the variation of impedance becomes too small to be useful. However, when the frequency is at 100 MHz, the effect is better than 500 MHz and 1 GHz, which is coincident with aforementioned, and operating at high frequency can cause shallow penetration depth. In practice, oil-based muds invade formations to depths of several inches or less in an LWD system, so this method can only measure the invasion zone.

3.3. Application Example

As an application example, we investigated the tool response in a three-layer formation with borehole, and the 3D model is shown in Figure 6. The coil and FDTD settings were the same as previously described. The upper and lower part were rock layer, with a conductivity of 10 S/m and a thickness of 300 mm. The center layer was the destination layer with a conductivity of 2 S/m and thickness of

Table 4. Electric and magnetic parameters for model plotted in Figure 6.

Material	Conductivity (S/m)	Permittivity
Rock	10	10
Destination	2	10
Mud	2	20
Steel	1.04e7	1
Coil	5.80e7	1

**Figure 6.** 3D model of a 3-layer inhomogeneous formation. This coil (with 20 turns, wire diameter of 4 mm and coil diameter of 7 cm) was directly dipped in the drilling liquid. The depth of the destination layer is 300 mm, and both the upper layer rock and the lower layer rock has a depth of 350 mm.

350 mm. Electrical and magnetic parameters of other materials are listed in Table 4. The simulation results are shown in Figure 7. The position under 350 mm and exceeding 650 mm means that the central point of the coil is in the rock layer. Similarly, the position exceeding 350 mm and under 650 mm means that the coil is in the destination layer. We can find that the real part of impedance increased as the coil entered the center layer, and the imaginary part of impedance decreased as the coil entered the center layer, which can be predicted by the results shown in Figure 4. So, the two kinds of formation with different conductivities can be distinguished by this method.

As Eq. (20) shows, the coil impedance can be calculated from the reflection coefficient $\Gamma(\omega)$, and the reflection coefficient is equal to S_{11} , so the coil impedance can be measured by using a vector network analyzer (VNA).

$$Z(\omega) = Z_0 \frac{1 + \Gamma(\omega)}{1 - \Gamma(\omega)} \quad (20)$$

Customarily, an accurate VNA meter is expensive and cumbersome, which is suitable for laboratory but not for the down-hole drilling. However, recent advances in electronic technology allow manufacturing one kind of network analyzer working at the lower frequency (kHz to GHz) with small size, which is suitable for working in the well-logging environment [22]. This kind of network analyzer uses direct digital synthesizer circuits to generate radio frequency test signal and local oscillation signal, and the intermediate frequency signal are sampled by Analog/Digital (A/D) converters. The digital data from A/D can be sent to a microprocessor for further processing and imaging. So, this kind of network

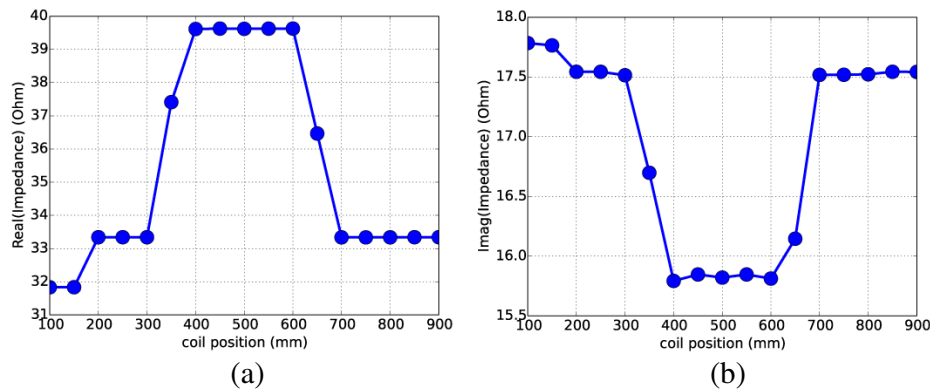


Figure 7. (a) real part (b) imaginary part of the impedance of the coil when it pass through a 3-layer formation, the operation frequency is 500 MHz.

analyzer can be very small and integrated in the printed circuit board for using in a well logging system, and it will be easy to obtain the impedance of the down-hole coil.

4. CONCLUSION

In this paper, a new well-logging method is proposed. We use this new method to obtain the formation conductivity by measuring the impedance of a metal coil. The curves of the coil impedance along with the formation conductivity at different frequencies were calculated using the FDTD method. The results showed that this method has good feasibility to be used in the LWD devices from 100 MHz to 1 GHz. To ensure the eddy current coil having enough penetration depth, we simulated the model with well bore diameter expanded from 80 mm to 100 mm. We also simulated a 3-layer formation well logging application and found that this method well distinguished the two kinds of formations. In summary, this work proposes a new method which is capable of measuring the formation conductivity in well-logging systems and is meaningful for providing reference in well logging field.

ACKNOWLEDGMENT

This work was supported by the China Postdoctoral Science Foundation (2012M511506). The authors would like to thank Dr. Edward C. Mignot, Shandong University, for linguistic advice.

REFERENCES

1. Sun, X. Y., Z.-P. Nie, A. Li, and X. Luo, "Analysis and correction of borehole effect on the responses of multicomponent induction logging tools," *Progress In Electromagnetics Research*, Vol. 85, 211–226, 2008.
2. Wait, J. R., "Complex resistivity of the earth," *Progress In Electromagnetics Research*, Vol. 1, 1–173, 1989.
3. Hasar, U. C., "Permittivity determination of fresh cement-based materials by an open-ended waveguide probe using amplitude-only measurements," *Progress In Electromagnetics Research*, Vol. 97, 27–43, 2009.
4. Lee, K. Y., B.-K. Chung, Z. Abbas, K. Y. You, and E. M. Cheng, "Amplitude-only measurements of a dual open ended coaxial sensor system for determination of complex permittivity of materials," *Progress In Electromagnetics Research M*, Vol. 28, 27–39, 2013.
5. Wang, B., K. Li, F. Kong, and S. Sheng, "Complex permittivity logging tool excited by transient signal for MWD/LWD," *Progress In Electromagnetics Research M*, Vol. 32, 95–113, 2013.

6. Anderson, B. I., *Modeling and Inversion Methods for the Interpretation of Resistivity Logging Tool Response*, Delft University Press, Delft, 2001.
7. Ellis, D. V. and J. M. Singer, *Well Logging for Earth Scientists*, Springer, Dordrecht, 2007.
8. Lee, H. O., et al., "Numerical modeling of eccentric LWD borehole sensors in dipping and fully anisotropic Earth formations," *IEEE Transactions on Geoscience and Remote Sensing*, Vol. 50, 727–735, 2012.
9. Tianxia, Z., M. Gerald, H. John, and C. G. Jaideva, "A novel technique to compute impedance of an arbitrarily oriented coil antenna for well logging applications," *2012 IEEE Antennas and Propagation Society International Symposium (APSURSI)*, Vol. 39, 2829–2838, 2012.
10. Theodoulidis, T. P., T. D. Tsiboukis, and E. E. Kriezis, "Analytical solutions in eddy current testing of layered metals with continuous conductivity profiles," *IEEE Transactions on Magnetics*, Vol. 31, 2254–2260, 1995.
11. Uzal, E., J. C. Moulder, S. Mitra, and J. H. Rose, "Impedance of coils over layered metals with continuity variable conductivity and permeability: Theory and experiment," *Journal of Applied Physics*, Vol. 74, 2076–89, 1993.
12. Uzal, E. and J. H. Rose., "The impedance of eddy current probes above layered metals whose conductivity and permeability vary continuously," *IEEE Transactions on Magnetics*, Vol. 29, 1869–1873, 1993.
13. Uzal, E., M. O. Kaya, and I. Zkol, "Impedance of a cylindrical coil over an infinite metallic half-space with shallow surface features," *Journal of Applied Physics*, Vol. 86, 2311–2317, 1999.
14. Theodoulidis, T. P. and J. R. Bowler, "Impedance of an induction coil at the opening of a borehole in a conductor," *Journal of Applied Physics*, Vol. 103, 024905, 2008.
15. Trltzsch, U., F. Wendler, and Kanoun, "Simplified analytical inductance model for a single turn eddy current sensor," *Sensors and Actuators A: Physical*, Vol. 191, 11–21, 2013.
16. Vasic, D., V. Bilas, and D. Ambrus, "Validation of a coil impedance model for simultaneous measurement of electromagnetic properties and inner diameter of a conductive tube," *IEEE Transactions on Instrumentation and Measurement*, Vol. 55, 337–342, 2006.
17. Vasic, D., V. Bilas, and B. snajder., "Analytical modelling in low-frequency electromagnetic measurements of steel casing properties," *NDT & E International*, Vol. 40, 103–111, 2007.
18. Hue, Y. K., F. L. Teixeira, L. E. S. Martin, and M. Bittar, "Modeling of EM logging tools in arbitrary 3-D borehole geometries using PML-FDTD," *IEEE Geoscience and Remote Sensing Letters*, Vol. 2, 78–81, 2005.
19. Taflove, A. and S. C. Hagness, *Computational Electrodynamics: The Finite-difference Time-domain Method*, Artech House, Boston, 2000.
20. Luebbers, R., L. Chen, T. Uno, and S. Adachi, "FDTD calculation of radiation patterns, impedance, and gain for a monopole antenna on a conducting box," *IEEE Transactions on Antennas and Propagation*, Vol. 40, 1577–1583, 1992.
21. TerMan, F. E., *Radio Engineers' Handbook*, McGraw-Hill, London, 1950.
22. De Mulder, B., K. Van Renterghem, E. De Backer, P. Suanet, and J. Vandewege, "Java-enabled low cost RF vector network analyzer," *The 3rd International IEEE-NEWCAS Conference*, 377–380, 2005.